

# Gravity wave interaction with a floating elastic plate in the presence of a pair of porous arc walls

Pawan Negi<sup>a</sup>, Trilochan Sahoo<sup>a</sup>, M. H. Meylan<sup>b</sup>

- a. Department of Ocean Engineering and Naval Architecture, Indian Institute of Technology Kharagpur, Kharagpur, 721302, India
  - b. School of Information and Physical Sciences, The University of Newcastle, Callaghan NSW 2308, Australia
- Email: pawan.negi04@gmail.com

## 1 Introduction

In recent times, there have been significant breakthroughs in the study of surface gravity wave interaction with very large floating structures (VLFS) of various forms and geometries. Additionally, these structures are proposed and constructed for floating airports, floating offshore bases, storage facilities, and sustainable uses of ocean space to promote the blue economy. Among floating structures of various configurations, circular structures are preferred for optimum utilisation of ocean space. Besides, circular structures can be easily extended without affecting various hydrodynamic characteristics due to structural symmetry. Furthermore, porous breakwaters are generally constructed to mitigate wave-induced forces on floating structures and create a calm zone in the vicinity of the floating facility. In recent years, arc-shaped porous structures have been proposed to improve protective effects and reduce the construction costs of complete porous cylindrical structures. Zhai et al. (2022) analysed the diffraction problem of the interaction of solitary waves with the combined asymmetric porous arc walls sheltering an impermeable cylinder. Further, a recent study depicts that flexural gravity wave blocking may occur when the floating elastic plate is under the action of higher lateral compressive stress. In such a situation, the blocking/saddle point occurs, where the dispersion relation possesses roots of multiplicity two/three for certain wave frequencies. Das et al. (2018) discovered that the dispersion relation of flexural gravity waves has three propagating wave modes within two different blocking points for certain fixed values of compressive force and frequency. In the present study, a mathematical model is developed to study the interaction of surface gravity waves with the dual porous arc-shaped bottom-mounted breakwater (ABBW) enclosing a circular floating elastic plate. The role of flexural gravity wave blocking in gravity wave interaction with a circular floating elastic plate is studied in the presence of a pair of porous arc walls. Fourier-Bessel series type expansion formulae are used to account for single as well as multiple propagating wave modes. Various hydrodynamic characteristics such as the hydrodynamic forces and moments acting on the arc walls and the elastic plate are analysed.

## 2 Mathematical Formulation and solution method

In the present study, a mathematical model is developed to study the interaction of surface gravity waves with the dual porous arc-shaped bottom-mounted breakwater (ABBW) enclosing a circular floating elastic plate. The physical problem is considered in a three-dimensional cylindrical polar coordinate system  $(r, \theta, y)$  with  $r - \theta$  being the horizontal plane and the  $y$ -axis acting vertically downward from the mean sea level, as shown in Fig. 1.

Further, it is assumed that the thickness of each ABBW is considered negligible to incident wavelength, and both the breakwaters are fixed rigidly at the sea bed and are extended till the free surface. The outer ABBW is symmetrically placed between  $\theta = \alpha_1$  and  $\theta = 2\pi - \alpha_1$  at a radial distance  $r = a$ , while the inner ABBW is placed at a radial distance  $r = b$  and between  $\theta = \alpha_2$  and  $\theta = 2\pi - \alpha_2$ . Thus, the central angles of the outer and inner ABBWs are  $\gamma_1 = 2\pi - 2\alpha_1$  and  $\gamma_2 = 2\pi - 2\alpha_2$ , respectively. In further consideration, a circular elastic plate with radius  $r = c$  is positioned to align its centre with the origin  $O$ . Therefore, the fluid domain is divided into four sub-domains:  $\Omega_j$  for  $j = 1, 2, 3, 4$ . Moreover, the water depth is assumed to be finite  $h$ , and the incident wave reaches the breakwaters, creating an angle  $\beta$  with the  $x$ -axis, as shown in Fig. 1. Furthermore, it is assumed that the elastic plate is thin, isotropic, and homogeneous and is acted on by the uniform lateral compressive force  $\mathcal{N}$ . Moreover, the fluid is assumed to be inviscid and incompressible, whereas the flow is considered to be irrotational and simple harmonic in time with angular frequency  $\omega$ . Thus, there exists a velocity potential and surface displacements of the forms  $\Phi_j(r, \theta, z, t) = \Re\{\phi_j(r, \theta, z)e^{-i\omega t}\}$  and  $\zeta_j(r, \theta, t) = \Re\{\eta_j(r, \theta)e^{-i\omega t}\}$  respectively. Thus, the spatial velocity potentials  $\phi_j$ s satisfy

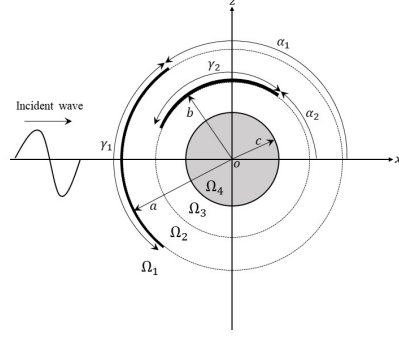


Figure 1: Schematic diagram of wave interaction with dual arc walls

where  $\nabla_{r\theta}^2 \equiv \partial_r^2 + (1/r) \partial_r + (1/r^2) \partial_\theta^2$ . The velocity potential  $\phi_j$  satisfies the linearized free surface condition in the open water region and the sea bed condition, as in Duan et al. (2012). Further, the linearized boundary condition in the circular plate-covered region is obtained as

$$(\nabla_{r\theta}^2 + \partial_y^2) \phi_j = 0, \quad \text{for } j = 1, 2, 3, 4, \quad (1)$$

where  $D = EI/\rho g$ ,  $Q = \mathcal{N}/\rho g$ ,  $m_s = \rho_i d/\rho g$  with  $E$  being the Young's modulus,  $I = d^3/12(1 - \nu^2)$  is the moment of inertia with  $d$  being the plate thickness,  $\nu$  is the Poisson's ratio,  $\rho_i$  is the structural density,  $\rho$  is the fluid density. Moreover, the continuity of pressure and velocity on the porous arc walls, along with the virtual dividing surface and the floating elastic plate for  $j = 1, 2, 3$  yields (Zhai et al. (2022))

$$(D\nabla_{r\theta}^4 + Q\nabla_{r\theta}^2 - m_s\omega^2 + 1) \frac{\partial\phi_4}{\partial y} = -\frac{\omega^2}{g}\phi_4 \quad \text{on } y = 0, \quad (2)$$

where  $D = EI/\rho g$ ,  $Q = \mathcal{N}/\rho g$ ,  $m_s = \rho_i d/\rho g$  with  $E$  being the Young's modulus,  $I = d^3/12(1 - \nu^2)$  is the moment of inertia with  $d$  being the plate thickness,  $\nu$  is the Poisson's ratio,  $\rho_i$  is the structural density,  $\rho$  is the fluid density. Moreover, the continuity of pressure and velocity on the porous arc walls, along with the virtual dividing surface and the floating elastic plate for  $j = 1, 2, 3$  yields (Zhai et al. (2022))

$$\phi_j = \phi_{j+1}, \quad \frac{\partial\phi_j}{\partial r} = \frac{\partial\phi_{j+1}}{\partial r}, \quad \text{on } r = a_j, \quad -\alpha_j \leq \theta \leq \alpha_j \quad \text{and} \quad 0 < y < h, \quad (3)$$

with  $a_3 = c$  and  $0 \leq \theta \leq 2\pi$ . Further, on the porous arc walls across the water depth  $0 < y < h$  (as in Duan et al. (2012))

$$\frac{\partial\phi_j}{\partial r} = \frac{\partial\phi_{j+1}}{\partial r} = iG_j k_0 (\phi_{j+1} - \phi_j) \quad \text{on } r = a_j, \quad \alpha_j \leq \theta \leq 2\pi - \alpha_j, \quad j = 1, 2. \quad (4)$$

Moreover, across the interface of the floating plate and open water, the continuity of pressure and velocity yields

$$\phi_3 = \phi_4, \quad \frac{\partial \phi_3}{\partial r} = \frac{\partial \phi_4}{\partial r} \quad \text{at } r = c, \quad 0 \leq \theta \leq 2\pi \quad \text{and} \quad 0 < y < h, \quad (5)$$

where  $k_0$  is the wavenumber associated with the plane incident progressive wave and  $G_j$  for  $j = 1, 2$  are the porous-effect parameters of the outer and inner walls. Besides, the elastic plate is assumed to be floating freely, which will yield the vanishing of the bending moment and shear force at the plate edge as in Mondal et al. (2014). Further, the velocity potential satisfies the far-field condition given by

$$\lim_{r \rightarrow \infty} \sqrt{r} \left\{ \frac{\partial(\phi - \phi_0)}{\partial r} - ik_0(\phi - \phi_0) \right\} = 0, \quad (6)$$

where  $\phi_0(r, \theta, y)$  is the spatial velocity potential associated with the incident plane progressive wave. In the subsequent discussion, we present the form of the velocity potentials using the Fourier-Bessel type expansion formula.

The spatial velocity potentials  $\phi_j(r, \theta, y)$  satisfy the governing equation Eq. (1) along with the boundary conditions as in Eqs. (2) and the far-field condition in Eq. (6) in finite water depth, are given by

$$\begin{aligned} \phi_1(r, \theta, y) = & \frac{-igH}{2\omega} \sum_{m=0}^{\infty} f_0(y) \epsilon_m \cos m(\theta - \beta) J_m(k_0 r) \\ & + \sum_{i=0}^{\infty} \sum_{m=0}^{\infty} f_i(y) \left( A_{m,i}^{(1)} \cos m\theta + B_{m,i}^{(1)} \sin m\theta \right) H_m^{(1)}(k_i r), \end{aligned} \quad (7)$$

$$\begin{aligned} \phi_j(r, \theta, y) = & \frac{-igH}{2\omega} \sum_{i=0}^{\infty} \sum_{m=0}^{\infty} f_i(y) \left( A_{m,i}^{(j)} \cos m\theta + B_{m,i}^{(j)} \sin m\theta \right) J_m(k_i r) \\ & + \sum_{i=0}^{\infty} \sum_{m=0}^{\infty} f_i(y) \left( C_{m,i}^{(j)} \cos m\theta + D_{m,i}^{(j)} \sin m\theta \right) H_m^{(1)}(k_i r) \quad \text{for } j = 2, 3, \end{aligned} \quad (8)$$

$$\phi_4(r, \theta, y) = \frac{-igH}{2\omega} \sum_{i=0, I, II, 1}^{\infty} \sum_{m=0}^{\infty} g_i(y) \left( A_{m,i}^{(4)} \cos m\theta + B_{m,i}^{(4)} \sin m\theta \right) J_m(p_i r), \quad (9)$$

where  $J_m(\cdot)$  and  $H_m^{(1)}(\cdot)$  are the Bessel function and Hankel function of the first kind of order  $m$  respectively and  $\epsilon_m$  being the same as defined earlier, whilst  $f_i(y)$ 's and  $g_i(y)$ 's are the vertical eigenfunctions with  $k_i$  and  $p_i$  being the corresponding eigenvalues in the open water and plate-covered regions respectively (Mondal et al. (2014)). Further,  $A_{m,i}^{(j)}$ ,  $B_{m,i}^{(j)}$ ,  $C_{m,i}^{(2)}$ ,  $D_{m,i}^{(2)}$ ,  $C_{m,i}^{(3)}$ , and  $D_{m,i}^{(3)}$  are the unknown complex constants which are to be determined. Using various conditions at the interface boundaries and edges of the plate and the orthogonal property of the trigonometric functions and vertical eigenfunctions in the open water region, a system of  $(4M + 2) \times (3N + 4)$  linear equations are derived after truncating the infinite series in  $m$  and  $i$  after  $M$  and  $N$  terms respectively, which is solved using MATLAB for computing various physical results of interest. Besides, the velocity potential  $\phi_4(r, \theta, y)$  will be generalized to account for multiple propagating wave modes during wave blocking and details will be discussed during the presentation.

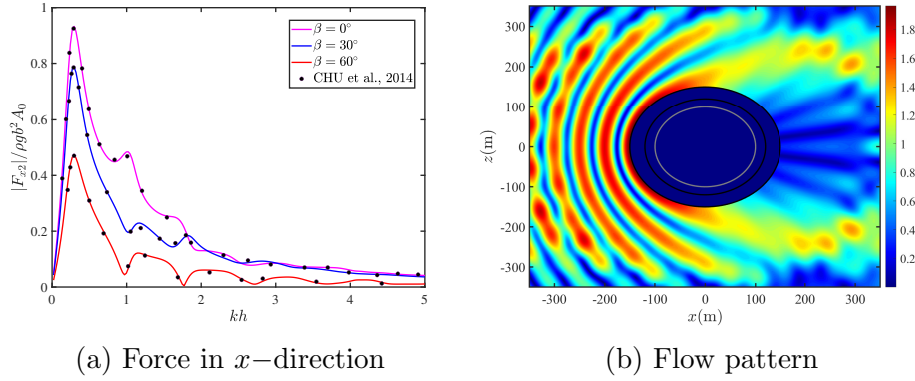


Figure 2: (a) Validation and (b) verification of the physical model.

### 3 Model validation

For validation of the numerical results, hydrodynamics forces acting on the breakwater are computed and compared with the known results of a single rigid arc-shaped bottom-mounted breakwater (Chu et al. (2014)). Various fixed parameters are considered as  $\alpha_1 = 180^\circ$ ,  $\alpha_2 = 120^\circ$ ,  $G_1 = G_2 = 0$ ,  $a = 150$  m,  $b = 100$  m and  $c = 50$  m,  $h = 20$  m,  $H = 2$  m. Further, the horizontal force  $|F_{x2}|/\rho g b^2 H$  as in Fig. 2a is plotted for different values of the incident wave angle  $\theta$ . A good agreement is observed between the present results and that of Chu et al. (2014) which depicts that our analytical model will be useful and effective for studying the present problem related to different parameters.

Subsequently, a pair of rigid cylinders is considered around the floating elastic disk under the porous condition  $G_1 = G_2 = 0$  and the angles  $\alpha_1 = \alpha_2 = 0^\circ$ . The flow distributions around the cylinders and the disk are exhibited in Fig. 2b. It is observed that the incident wave is diffracted around the outer cylinder and that there is no wave or plate excitation in the annular region between the two cylinders. Moreover, various results on the role of the arc-shaped breakwaters in mitigating the wave-induced forces on the floating plate will be presented in the workshop.

### References

- Chu, Y. C., Cheng, J. S., Wang, J. Q., Li, Z. G. & Jiang, K. B. (2014), ‘Hydrodynamic performance of the arc-shaped bottom-mounted breakwater’, *China Ocean Engineering* **28**, 749–760.
- Das, S., Sahoo, T. & Meylan, M. H. (2018), ‘Dynamics of flexural gravity waves: from sea ice to hawking radiation and analogue gravity’, *Proc Roy Soc Ser A* **474**(2209), 20170223.
- Duan, J., Cheng, J., Wang, J. & Wang, J. (2012), ‘Wave diffraction on arc-shaped floating perforated breakwaters’, *China Ocean Engineering* **26**(2), 305–316.
- Mondal, R., Mandal, S. & Sahoo, T. (2014), ‘Surface gravity wave interaction with circular flexible structures’, *Ocean engineering* **88**, 446–462.
- Zhai, Z., Zheng, S. & Wan, D. (2022), ‘Interaction between solitary waves and a combined structure of two concentric asymmetric porous arc walls’, *Physics of Fluids* **34**(4).